EAST EUROPEAN JOURNAL OF PHYSICS. **1.** 47-57 (2022)
DOI:10.26565/2312-4334-2022-1-07 ISSN 2312-4334

STUDY OF STRUCTURAL, ELASTIC, THERMAL AND TRANSPORT PROPERTIES OF TERNARY X(X=Co, Rh and Ir)MnAs OBTAINED BY DFT†

Salim Kadri[a], Tourab Mohamed[b], Berkani Mahièddine[c], Amraoui Rabie[d], Bordjiba Zeyneb[d]
[a]*Dynamic Motors and Vibroacoustic Laboratory, M'Hamed Bougara University of Boumerdes*
[b]*Faculty of Technology, M'Hamed Bougara University, Cité Frantz Fanon, Boumerdes 35000-Algeria*
[c]*LSELM Laboratory, Badji Mokhtar Annaba University, Annaba 23000, Algeria*
[d]*Material Physics Laboratory - L2PM, 8 May 1945 University of Guelma, Algeria*
**Corresponding Author: amraoui.rabie@yahoo.com*
Received January 14, 2022; revised February 23, 2022; accepted March 16, 2022

The Density Functional Theory (DFT) with an approximation of generalised gradient is used for the study of elastic, thermodynamic and transport properties and for that of structural stability of ternary Half-Heuslers compounds X(X=Co, Rh and Ir)MnAs. This first predictive study of this compounds determines the mechanical properties such that the compression, shearing, Young modulla and Poisson coefficient without omitting the checking parameters of the nature of these compounds such that hardness, Zener anisotropic facto rand Cauchy pressure. The Pugh ratio and Poisson coefficient have allowed the identification of ductile nature of these compounds. The speed of sound and Debye temperature of these compounds has also been estimated from the elastic constants. The thermodynamic properties have been calculated as well for a pressure interval from zero to 25 GPa. The effect of chemical potential variation on Seebeck coefficient, electric, thermal and electronic conductivities, the power and merit factors have also been studied for different temperatures (300, 600, 900°K), so that these alloys can be better potential candidates for thermoelectric applications.
Keywords: Half-Heusler, DFT, elastic, thermoelectric, transport properties
PACS: 71.15.Mb; 71.20.-b; 71.55.Ak; 72.20.Pa

The big challenge of material science specialists is to be able to produce new semi conductor materials with the best properties allowing them to be used in diverse applications. The ternary material of half-Heusler type is compound family showing several qualities such that elastic stability, high melting temperature high thermoelectric power factor and other stable thermal properties.

These material qualities make of these materials the best candidates to be used in several system manufacturing such as the Micro Electro Mechanical Systems (MEMS), dedectors and sensors of high accurency. These compounds known through their best thermoelectric properties are chemically presented by XYZ where X, Y corresponding to transition elements and Z to group elements III, IV or V [1].

Since their discovery by R.A Groot et al [2] the thermoelectrical HH compounds are known through their merit factor which indicates their ability to convert the lost heat to electricity. The ZT indicator is also a performance characteristic of this type of materials. The present challenge for the scientists is to look for the best Peltier and Seebeck effect efficiency. We seek to minimize the important volumes of exploitable natural resources in energy conversion to get a cost-effective utilization corresponding to the best power factors.

Many theoritical [3,4,5] and experimental [6,7] studies on the transport properties of HH compounds have been recently published. Among these works Ma et al [8] who by using DFT calculation they were be able to predict the structural, magnetic and electronic properties of of CoVX (X = Ge et Si) compounds. In their remarkable work, Ahmed et al [9], an artificial neural network model has been developed to predict the network constants of 137 HH compounds.

This work is considered as the most reliable reference for the network constants of several HH compounds. Moreover the work of Chibani et al [10], whose process has been as guide for the present work have used a DFT calculation to determine the structural, electronic and transport properties of HH CoVX (X=Ge and Si) compounds whose elastic stability has been verified.

The aim of the present work is by using ab initio calculation, to study the structural, elastic and thermoelectric properties of X(X=Co, Rh and Ir) MnAs materials. First, a verification of both structural state and elastic stabilities of the compounds is done. Then, using the power of Gibbs and Boltztrap calculation codes the Debye and Boltzman quasi harmonic equations are solved. The solutions of these equations determine and illustrate some thermodynamic transport parameters such as Seebeck coefficient, electric, thermal and electronic conductivities, the power and merit factor.

Some results of the study such as elastic, thermal and transport properties of X(X=Co, Rh and Ir)MnAs half-Heusler compounds will be used for the analysis by finite elements of the MEMS driver behavior.

COMPUTATIONAL METHOD

In this work the WIEN2K [11] package has been used for the calculation in theoretical DFT domain [12]. This package has been used to calculate the electronic structure of (X=Co, Rh and Ir)MnAs compounds, in cubic phase using Augmented Planes Waves method (FP-LAPW) exploiting generalized gradient approximation (GGA-WC) for exchange

† ***Cite as***: S. Kadri, T. Mohamed, B. Mahièddine, A. Rabie, and B. Zeyneb, East. Eur. J. Phys. **1**, 47 (2022), https://doi.org/10.26565/2312-4334-2022-1-07

energy and correlation. The number of particular k points used the irreducible Integration in Brillouin zone is 3000. The value of density plane cut-off is RKmax equal to 8 for energy eigen values and eigen vectors of these points.

Generally the half-Heusler X(X=Co, Rh and Ir)MnAs crystallize in $C1_b$ structure in cubic phase Fig.1 in a way that the atoms X(X=Co, Rh and Ir) occupy 4a (0.25, 0.25, 0.25) sites. The Mn atom occupies 4b (0.5, 0.5, 0.5) site and, As atom occupies the site 4c (0, 0, 0) in Wyckoff coordinates [13].

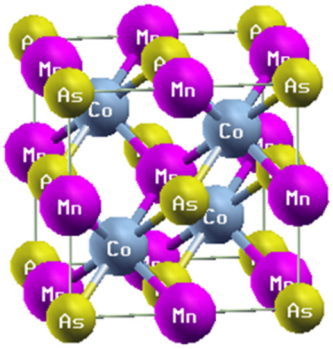

Figure 1. Half Heusler compound Structure.

RESULTS AND DISCUSSION

Structural stability

The study of materials structural properties of X(X=Co, Rh and Ir)MnAs is to determine at static equilibrium, the material structure parameters such as the mesh parameters a_0, the compression modulus B and its derivative B'. By using the total quantities of energies as function of volume at the equilibrium. The present study is for predicting the more stable phase of the compounds using the state equation of Murnaghan [13].

$$E(V) = E_0 + \frac{B}{B'(B'-1)}\left[V\left(\frac{V_0}{V}\right)^{B'} - V_0\right] + \frac{B}{B'}(V - V_0)$$

Where E_0, B and V_0 are respectively: total energy, compression modulus and the volume at the equilibrium.

An auto coherent calculation has been carried out to determine the total energy of X(X=Co, Rh and Ir)MnAs ternary compounds in two phases: non magnetic named MN, and ferromagnetic named FM of space group (216_F43m). The total energy evolution as function of volume mesh in phase MN and FM is depicted on the same curve (Figure 2) in order to provide evidence of the lowest energy.

The Figure 2 shows that the most stable structure among the three studied materials are that of ferromagnetic of cubic structure of X(X=Co, Rh and Ir)MnAs materials and that of 216_F43m space group. The Table 1 shows the parameter values of a_0 mesh, compression modulus B and its derivative B' of the same X(X=Co, Rh and Ir)MnAs compounds in the most stable ferromagnetic phase.

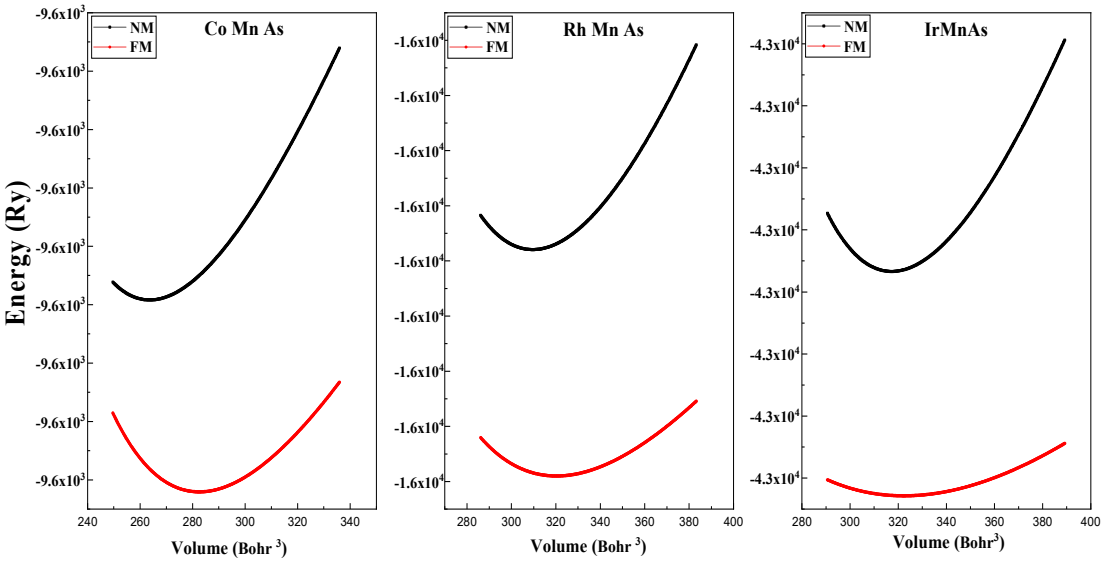

Figure 2. Optimisation of tatal energy of X(X=Co, Rh et Ir)MnAs compounds for all structure types

Table 1. Fundamental state properties of X(X=Co, Rh et Ir)MnAs half-Heuslers

	Constante de réseau a_0(Å)			Module de compression B (GPa)		La dérivée de B' (GPa)	
	Notre travail	Exp	Autre calcul	Notre travail	Autre calcul	Notre travail	Autre calcul
CoMnAs	5.468	-	5.53[9]	164.279	-	5.470	-
RhMnAs	5.768	-	5.83[9]	162.842	-	6.456	-
IrMnAs	5.810	-	-	179.849	-	5.239	-

Elastic Properties

The study aim of the mechanical behaviour of materials is to determine their response to a given Stress. In physics, elasticity is the capacity of a material to regain its initial geometry after suppression of applied forces. The elastic constraints C_{ij} have been calculated by Thomas Charpin method [14] incorporated in Wien2k code.

Because of the lack of data in the literature, all X(X=Co, Rh and Ir)MnAs alloys C_{ij} are calculated and put in Table 2. The calculated elastic constants $C_{44} > 0$, $C_{11} - C_{12} > 0$ and $C_{11}+2\,C_{12} > 0$, with C_{12} less than C_{11}, respect the criteria of Born-Huang relative to mechanical stability [15]. These constants respect the cubic stability condition too i.e. $C_{12} < B < C_{11}$. This is confirming that the alloys are elastically stable.

Table 2. Calculated values of elastic constants for X(X=Co, Rh and Ir)MnAs compounds.

Elasticity cofficients	CoMnAs	RhMnAs	IrMnAs
C_{11}(GPa)	164.4	262.2	195.6
C_{12}(GPa)	126.4	76.2	122.2
C_{44}(GPa)	72.3	71.6	74.5

To describe the mechanical behaviour of these materials on the basis of C_{ij} constants the elastic amounts such as shearing modulus G, the Young modulus E and the Poisson ν ratio are evaluated using Voigt-Reuss-Hill approximation [16] at the equilibrium for a pressure P = 0.

In the following the indices R and V of the shearing modula are relative respectively to Voigt and Reuss approximation. For the cubic systems these elastic quantities are calculated using the following expressions:

$$B = \frac{C_{11} + 2C_{12}}{3}$$

$$G = \frac{G_V + G_R}{2}$$

$$G_V = \frac{\left(C_{11} - C_{12} + 3C_{44}\right)}{5}$$

$$G_R = \frac{5C_{44}\left(C_{11} - C_{12}\right)}{4C_{44} + 3\left(C_{11} - C_{12}\right)}$$

$$E = \frac{9BG}{\left(3B + G\right)}$$

$$\nu = \frac{3B - E}{6B}$$

The obtained results of this work compounds are given in Table 3. It should be noticed that the theoretical values are not available in the literature. The compressibility modulus B gives information on the hardness of the material; the more B is large the more the material is hard.

Table 3. Compression Modulus (B) GPa, Shearing modulus (G) GPa, Young modulus(E) GPa, Poisson Coefficient (ν), the ratio B/G , The micro hardness (H), the l'anisotropy A , Cauchy CP coefficients The volumetric mass ρ in Kg/m^3 , Fusion Temperatures (T_m) in °K.

Materials	B	G	E	ν	B/G	H	A	CP	ρ	$T_m \pm 300$
CoMnAs	139.06	42.52	115.76	0.36	3.27	3.33	3.8	54.1	5561.31	1300.15
RhMnAs	138.2	63.08	164.25	0.30	2.19	6.94	0.77	4.6	6041.4	1003.41
IrMnAs	146.67	56.07	149.19	0.33	2.61	5.14	2.03	2.03	8179.7	1275.32

The compressibility modulus values determined for these half- Heusler are large (B > 30 GPa); This implies these alloys have weak compressibility [17], consequently, these alloys can be classified as relatively hard and able to resist to volume and shape changes in ambient conditions.

It should be noticed that the shearing modulus of considered alloys is much weaker than that of compressibility one. This points out that these alloys are susceptible rather to resist to volume compression than to shape variation.

Knowing that Pugh (B/G) ratio [17] permits the distinction of the ductility when ($B/G \geq 1.75$) and fragility in the opposite case. The values of (B/G) on Table 3 shows well the ductility of the studied materials. The Poisson coefficient can also be used as indicator of the ductility, fragility of an alloy.

In general, it is equal or greater than 1/3 for ductile materials and smaller than this value for fragile materials. In this study the Poisson coefficient of half-Heusler compounds is greater than 1/3. This confirms these compounds ductility as it was determined previously.

The Young modulus E characterises a given material rigidity. When its Young modulus increases, this material becomes rigid. The calculated values of E for considered materials are less elevated. This points out that their rigidity is more or less elevated.

In this work the hardness of these alloys is calculated as well. This mechanical property gives information on the elasticity, the plasticity and the rupture of these alloys. In the literature many methods are used for hardness calculations. In the present work the Vickers micro- hardness model has been adopted. The Vickers hardness is determined by the following Tian et al equation [18]:

$$H_V = 0.92.\left(\frac{G}{B}\right)^{1.137} \cdot G^{0.703}$$

From Table 3 it can be shown that the alloys present a weak hardness. So they cannot withstand large loads. These materials cannot be recommended for electronic and mechanical small spares manufacturing.

On the other hand, the elastic constant knowledge has permitted the deduction of other mechanical characteristics such as the anisotropy A , the coefficient of Cauchy CP and the fusion temperature.

To know if a material is isotropic or anisotropic the value of Zener anisotropy factor should first be known. This factor measures the solid anisotropy degree. The material is perfectly isotropic if $A = 1$ and anisotropic if $A \neq 1$ This Zener factor is determined by the following equation [19]:

$$A = \frac{2C_{44}}{(C_{11} - C_{12})}$$

The three studied compounds have anisotropic factors (A different of 1), therefore, they are anisotropic. If the Zener coefficient, $A\rangle 1$ then it is maximal rigidity case along the diagonal of the cube <111>. It's the case of CoMnAs and IrMnAs compounds.

In opposite way if A<1 the isotropy is maximal along the axis of the cube <1 0 0> it is the case of RhMnAs compounds. To see whether the character of the atomic bound is fragile or ductile among the metals and the compounds, the pressure of Cauchy CP [20] should determined as:

$$CP = C_{12} - C_{44}$$

For the present work alloys the pressure value of Cauchy is positive. This means that the metallic characters of these compounds are of ductile nature. Moreover, the alloy fusion temperature can be determined from the elastic constants using the following equation [21]:

$$T_m(°K) = \left[553 + (5.911)C_{12}\right] \pm 300$$

Debe temperature (θ_D) offers many information on the solid material undergoing temperature effect during its exploitation. (θ_D) is also related to the upper limit of photon frequencies. It is calculated as function of elastic constants according to the following equation:

$$\theta_D = \frac{h}{k_B}\left[\frac{3}{4\pi}\left(\frac{N_A\rho}{M}\right)\right]^{\frac{1}{3}} V_m$$

With N_a Avogadro number; the molar mass, the volumetric mass; h the Planck constant; the Boltzmann constant; the mean sound speed. This latter can be expressed as:

$$V_m = \left[\frac{1}{3}\left(\frac{2}{V_t^3} + \frac{1}{V_l^3}\right)\right]^{-\frac{1}{3}}$$

where: $V_l = \left(\frac{3B+4G}{3\rho}\right)^{\frac{1}{2}}$, $V_t = \left(\frac{G}{\rho}\right)^{\frac{1}{2}}$, V_l Represent the longitudinal propagation of sound velocity, and V_t its transversal velocity.

The velocities of sound propagation and the Debye temperature are put in Table 4:

Table 4. Longitudinal propagation sound velocity (m/s), Transversal propagation sound velocity (m/s), mean sound velocity (m/s), Debye Temperature (°K).

	V_l	V_t	V_m	θ_D
CoMnAs	5833.8	2718.9	3061.6	244.81
RhMnAs	6066	3231.3	3610.2	314.66
IrMnAs	5202.9	2618.2	2936	315.46

Thermal properties

Thermal properties of X(X=Co, Rh and Ir)MnAs compounds have been determined using quasi harmonic model of Debye [22]. This approximation put in action in Gibbs code is compatible with the Wien2k code.

This code has the merit to display several thermodynamic parameters at different temperatures and pressures such as heat capacity, Deybe temperature thermal expansion, entropy, enthalpy….etc.

Thermal quantities calculation as function of pressure and temperature, of X(X=Co, Rh and Ir)MnAs compounds, using quasi harmonic Debye model. This latter uses as input data in Gibbs program the *E-V* data of the primitive cell. *E-V* stands for total energy *E* and volume *V*.

The heat capacity at constant pressure C_p, the heat capacity at constant volume C_v, and the thermal expansion coefficient α are determined and presented in the temperature range of temperature (0 to 900 °K) and of pressure (0 to 25 GPa) .

Debey model parameters targeted here are respectively θ_D, the heat capacity at constant volume C_v, and the thermal expansion coefficient α [23,24]:

$$\theta_D = \frac{\hbar}{\mathrm{k}}\left[6\pi^2 V^{\frac{1}{2}} n\right]^{\frac{1}{3}} f(\nu)\sqrt{\frac{B_S}{M}}$$

$$C_V = 3nk_B\left[4D\left(\frac{\theta}{T}\right) - \frac{\frac{3\theta_D}{T}}{e^{\frac{\theta}{T}}-1}\right]$$

$$\alpha = \frac{\gamma C_V}{B_T V}$$

Where *M* is the molar mass; B_s is the adiabatic compression modulus, which is by the static compressibility.

$$B_S \cong B(V) = V\frac{d^2E(V)}{dV^2}$$

$f(\nu)$ est donnée par :

$$f(\nu) = \left\{3\left[2\left(\frac{2}{3}\frac{(1+\nu)}{(1-2\nu)}\right)^{3/2} + \left(\frac{1}{3}\frac{(1+\nu)}{(1-\nu)}\right)^{3/2}\right]^{-1}\right\}^{1/3}$$

ν is Poisson coefficient and γ is Grüneisen parameter.

The Figure 3 curve giving the thermal expansion coefficient α shows the three materials have sensibely identical behaviour for the same variations of temperature and pressure. α increases with the increase of the temperature, but decreases considerably with the increase of pressure.

It should be noted that the increase of the pressure weakens α growth with the temperature as it is shown clearly on Figure 3. It should be emphasized as well that α of CoMnAs compound presents the largest value compared to other compounds for a given temperature and pressure.

Let at T = 300 °K and P = 0 GPa, the thermal expansion coefficient be equal to 3.2805 (10^{-5} °K^{-1}), 2.5559 (10^{-5}°K^{-1}), 2.858 (10^{-5} °K^{-1}) for CoMnAs, RhMnAs, IrMnAs compounds respectively.

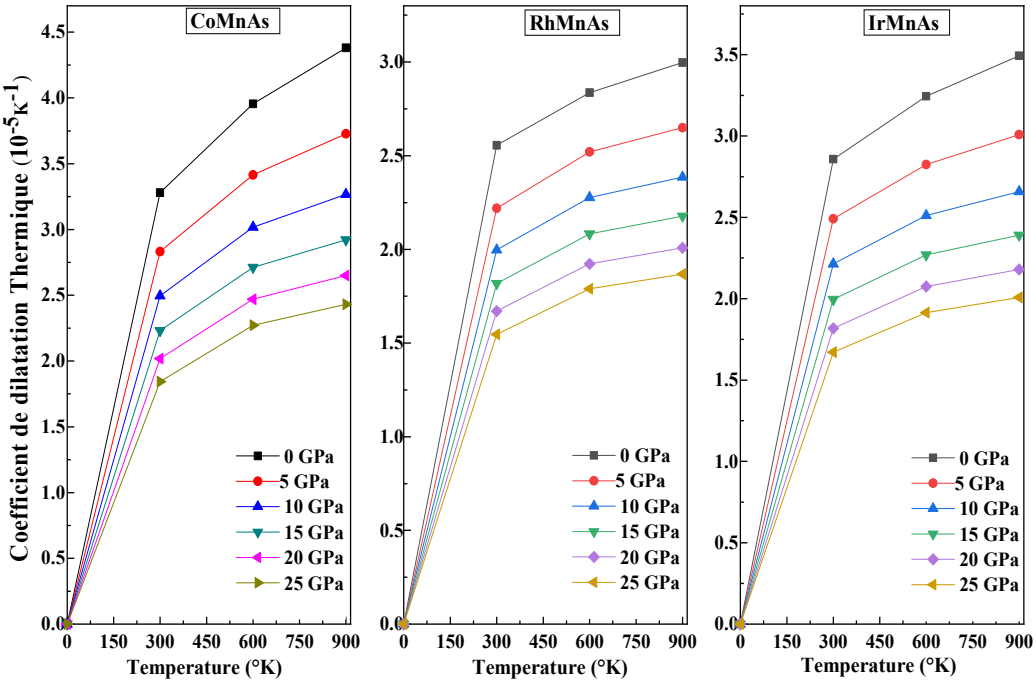

Figure 3. Thermal dilatation coefficient variation as function of temperature and pressure for XMnAs (X=Co, Rh et Ir) compounds.

The specific heat C_p expresses the energy or the photon number needed to increase the temperature of the material by one degree K [12]. C_p represents the change in temperature of thermal excitement energy U, associated to lattice vibrations. The Figure 4 representes the evolution of thermal capacity C_p at constant pressure as function of temperature at different pressure.

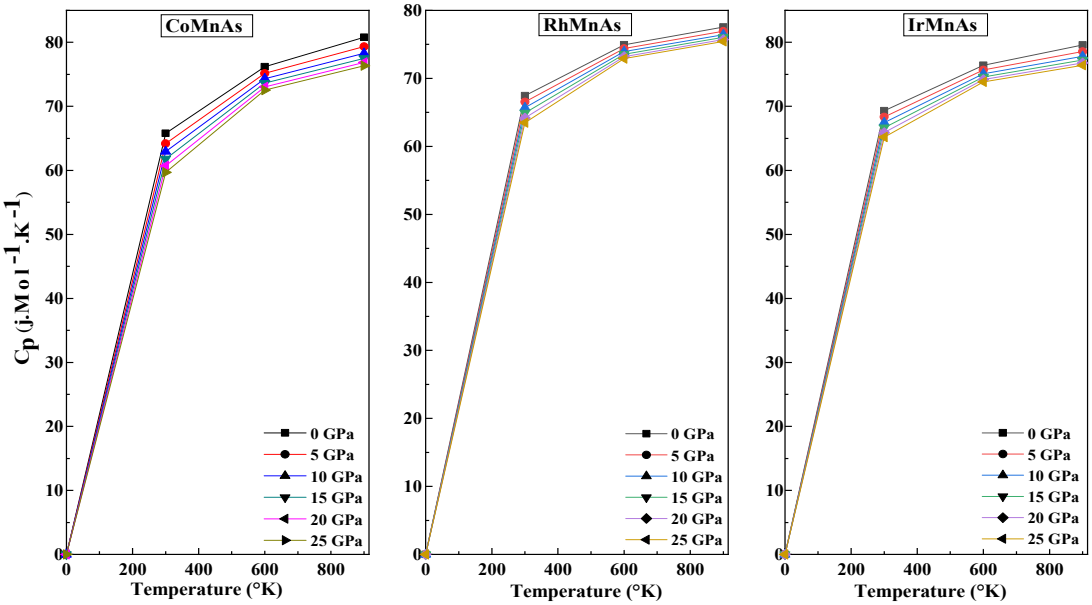

Figure 4. Calorific capacity (Cp variation as function of temperature at different pressures for) XMnAs (X=Co, Rh and Ir) compounds.

The results show, for the three half Huslers that the curves are nearly superimposed. This confirms that the pressure increase has no effect on C_p value. The heat capacity at constant pressure increases with an obvious monotony when temperature increases and converge towards a constant value. Thus, at high temperature this heat capacity could be thaught as constant. This hypothesis will be used in the following thermoelectric properties calculation.

The heat capacity C_v characterizes the material aptitude to store heat. C_v evolution as function of temperature in a pressure going from 0 to 25 GPa is shown on Fig. 5. For temperature less than 450 °K, C_v depends on temperature and pressure because of lack of harmony, beyond a certain temperature, C_v shows a horizontal profile and the differences between the thermal capacities at different pressures become more and more discrete with the temperature increase.

The heat capacity C_v decreases with pressure increase and increases with temperature increase. This implies that the temperature and the pressure have opposite effect with more impact of temperature compared to that of the pressure.

C_p and C_v values of the three compounds are nearly of the same order of magnitude. They are purely theoretical because none of the experimental data is available.

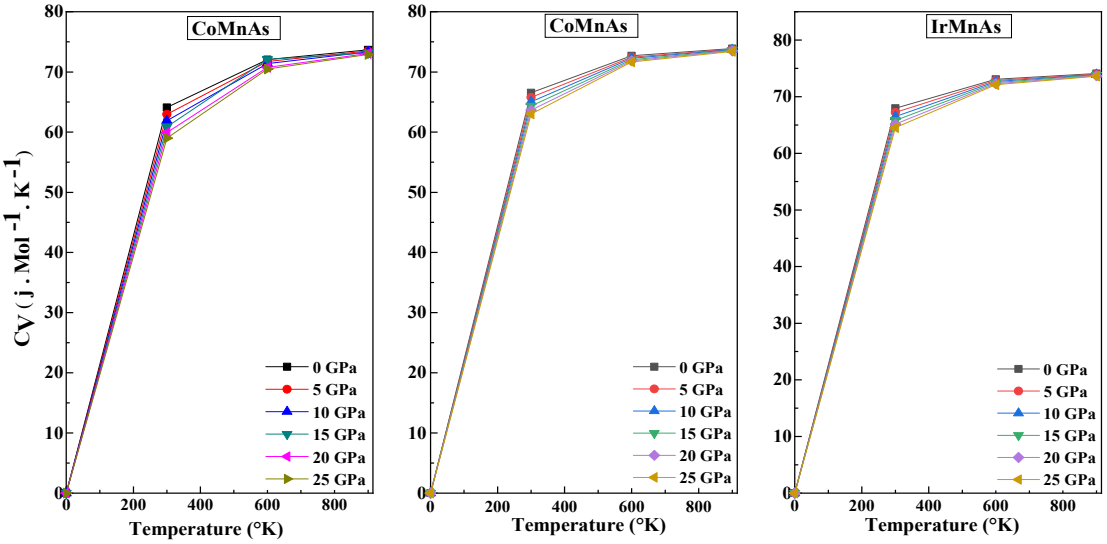

Figure 5. Calorific capacity (Cv variation as function of temperature at different pressures for (XMnAs (X=Co, Rh and Ir) compounds;

Transport properties

By keeping the diffusion time constant, the thermoelectric properties have been determined by using the semi classic theory of Boltzmann [25], as it was used in BoltzTraP code [26]. To get electronic and transport properties, including electric conductivity, Seebeck coefficient and electronic and thermal conductivities, the calculated band structure are given as input data in BoltzTraP package.To calculate the X(X=Co, Rh and Ir)MnAs compounds thermoelectric properties the calculated band structure has been used by WC-GGA approximation.

The Seebeck coefficient $S_{\alpha\beta}$, electrical conductivity σ and the tensors of electronic transport and thermal conductivity are expressed as follows k [27,28]:

$$S_{\alpha\beta}(T,\mu)=\frac{1}{eT\sigma_{\alpha\beta}(T,\mu)}\int\sigma_{\alpha\beta}(\in).(\in-\mu)^2\left[-\frac{\partial f_0(T,\in,\mu)}{\partial\in}\right]$$

$$\sigma_{\alpha\beta}=\frac{1}{\Omega}\int\sigma_{\alpha\beta}(\in)\left[-\frac{\partial f_0(T,\in,\mu)}{\partial\in}\right].d\in$$

$$k^0_{\alpha\beta}(T,\mu)=\frac{1}{e^2T.\Omega}\int\sigma_{\alpha\beta}(\in).(\in-\mu)^2\left[-\frac{\partial f_0(T,\in,\mu)}{\partial\in}\right].d\in$$

Where: e is the electro charge, Ω is the reciprocal space volume, $\in$ is the bearing energy, is the Fermi distribution function, μ is the chemical potential and T is the absolute temperature.
The conductivity tensor $\sigma_{\alpha\beta}(\in)$ as function of energy and electronic and thermal energy k ,is expressed as follows

$$\sigma_{\alpha\beta}(\in)=\frac{1}{N}\sum_{i,k}\sigma_{\alpha\beta}(i,k)\frac{\delta(\in-\in_{i,k})}{d\in}$$

Where N is the number of k-points.

It is well known in semi-conductors materials domain that in a p-type semi-conductor the majority charge carriers are holes and minority charge carriers are electrons.

In n type semi-conductor, the electrons are the majority charge carriers and the holes are the minority charge carriers [29]. On Figure 6 it is shown the Seebeck coefficient variation as function of the chemical potential varying between $\mu-E_F=\pm 2eV$ (considered as charge carrier concentration for the alloys) at different constant temperatures (300, 600 et 900 °K), in case of X(X=Co, Rh and Ir)MnAs [30] half-Husler compounds.

The negative characterisric of S indicates the n-type conduction, with the electrons as main charge carriers. Whereas the positive sign of S implies the p-type conduction with holes as majority carriers.

For the three compounds, the optimal values of S are obtained around Ef because S is inversely proportional to electrical conductivity and since in this region the conduction is intrinsic, therefore the conductivity is weak. These optimal values decrease when the temperature increases (Figure 6).

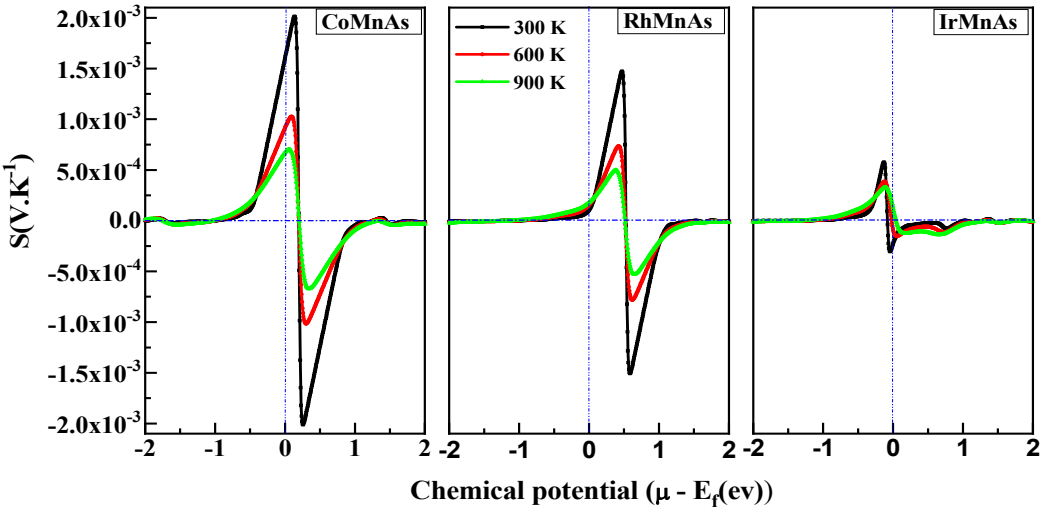

Figure 6. Seebeck coefficient S as function of chemical potential μ .

In case of CoMnAs and RhMnAs compounds, when $\mu = E_F$, the value of S is positive and the conduction is of p-type. So,these half-Heusler compounds are semi-conductors of p-type. On the contrary, for IrMnAs compounds, the value of S is negative in the level $\mu = E_F$, this entails that the conduction is of n-type and in this case, the compound is a semi-conductor of n- type.

On Figure 6, the peaks of CoMnAs compound are very important compared to the other peaks among them the IrMnAs compound is representing the weakest peaks.

The Figure 7 shows the electric conductivity variation as function of chemical potential $\mu - E_F = \pm 2eV$ at different temperatures (300°K, 600°K et 900°K). This curve shows the temperature effect on the electric conductivity is weak for the three considered compounds.

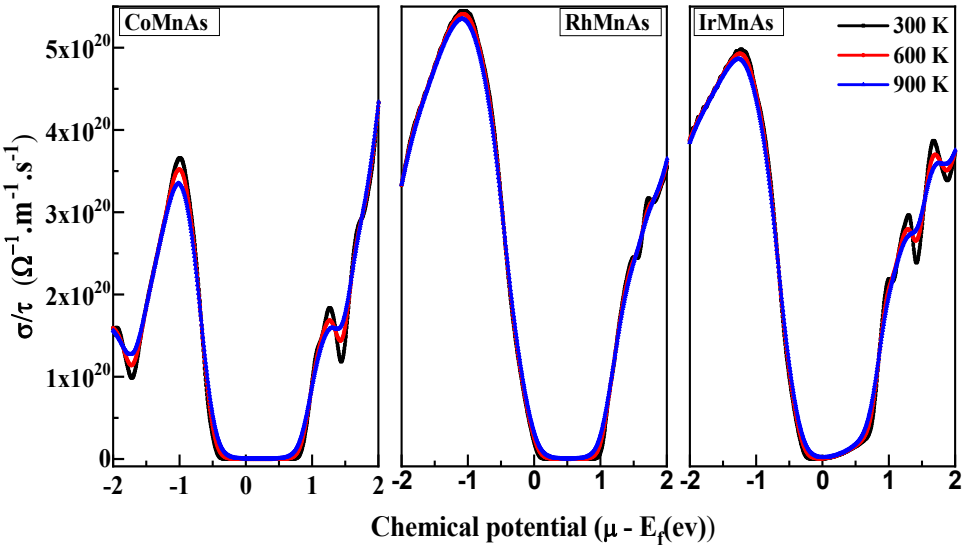

Figure 7. Electrical conductivity σ / τ as function of chemical potential μ .

For CoMnAs compound the n-type conductivity ($\mu \rangle E_F$) is greater than that of p-type ($\mu \langle E_F$). This is due to the difference between the electrons and holes mobility. On the contrary, for RhMnAs et IrMnAs compounds, the n-type conductivity is less than that of p-type.

The three main zones are well illustrated on Figure 7, the first zone when $\mu \langle E_F$ where the electric conductivity diminishes for the three compounds becoming intrinsic under the effect of the charge carriers (holes) concentration decrease at the vicinity of the chemical potential.

The electric conductivity diminishes for the three compounds. These latter become intrinsic under the decrease of charge carriers (holes) concentrations at the vicinity of the chemical potential.

In second zone corresponding to $\mu = E_F$ the electric conductivity becomes weaker with feeble charge carriers concentration, the last zone where $\mu \rangle E_F$ the charge carriers which are electrons will increase with chemical potential increase. And this leads to an electric conductivity.

Concerning the electronic thermal conductivity, Figure 8, it is clearly observed that the temperature rise increases significantly the electronic thermal conductivity of the three compounds. It is also noticed that the rise in temperature and the tendency of the electronic thermal conductivity are similar to that of the electric conductivity, having in mind that the charge carriers are also heat carriers [31].

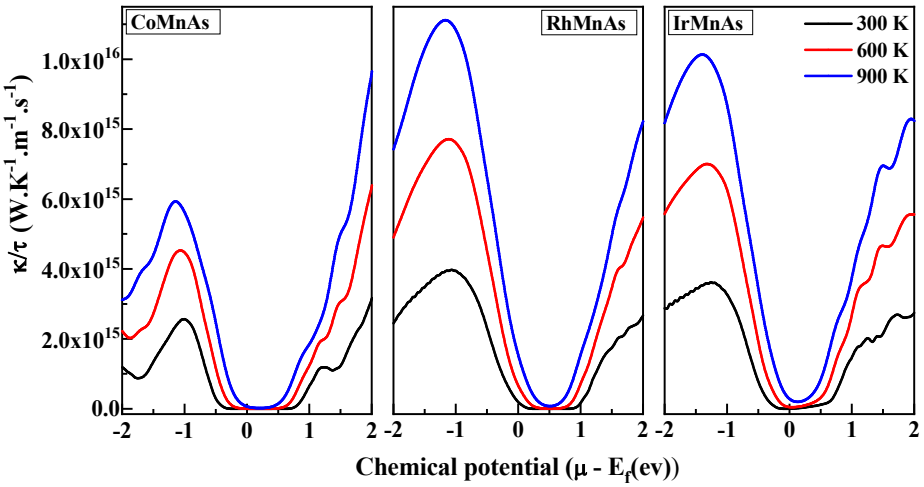

Figure 8. Electronic thermal conductivity k/τ as function of chemical potential μ

The qualities of a thermoelectric material is measured by a dimensionless number called merit factor i.e. the improvement in the material thermoelectric performance could be obtained through its merit factor ZT [32,33] expressed by:

$$ZT = \frac{S^2\sigma}{k_e + k_l}T$$

Where T is absolute temperature absolute, S the Seebeck coefficient, σ the electric conductivity, k_e the electronic thermal conductivity and k_l the lattice thermal conductivity.

To ensure whether the system could withstand higher temperatures the merit factor variations has been calculated as function of the chemical potential and this for an extended temperature range.

On Figure 9, ZT is maximal at only 300°K at the peaks, but as far as ZT takes the allure of fall starts its fall the highest temperature (900°K) becomes dominant with regard to the temperature of 300°K for the three compounds.

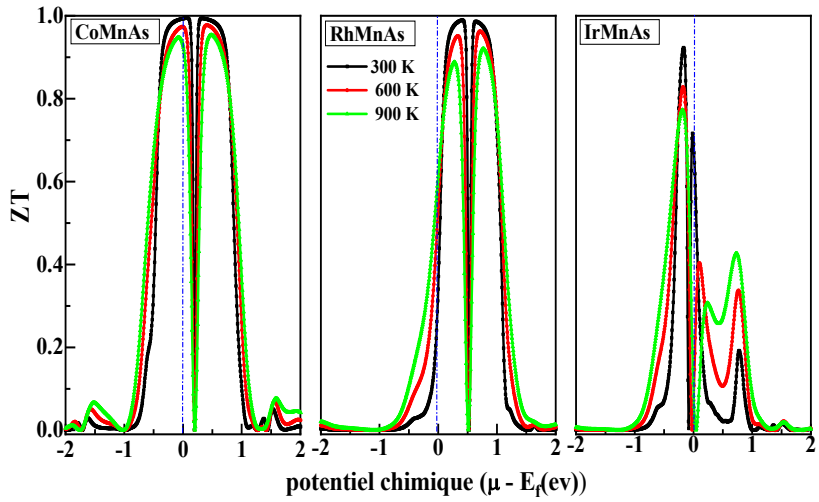

Figure 9. Merit factor (ZT) as function of chemical potential μ .

The merit factor of CoMnAs and RhMnAs compounds is close to the unit at ambient temperature. This makes of these alloys good candidates for thermoelectric apparatuses.

The small values of merit factor associated to IrMnAs half-Heusler are due to small values of Seebeck coefficient, to the electric conductivity, and to the increased values of the thermal conductivity too.

The Figure 10 represents the power factor PF, as function of the chemical potential where it can be noticed that PF increases with the temperature rise. It reaches a maximal value at T=900°K for the three compounds.

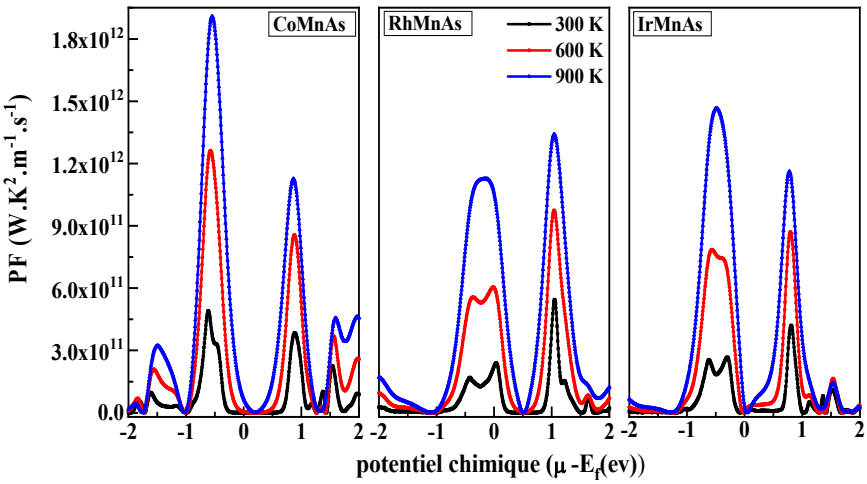

Figure 10. Power factor (PF) as function of chemical potential μ .

Two peaks of high intensity are also observed. One of them is a main peak near the Fermi level limit $\mu - E_F = -0.55, et - 0.48$ respectively for the X(X=Co, Ir)MnAs compounds for respectively, the values of $1.899.10^{12}$, and $1.46.10^{12}$ W/Mk^{2}s. contrarily, the principal peak of the RhMnAs compound comes after Fermi level, precisely at $\mu - E_F = 1.048$ with a value of PF= $1.335.10^{12}$ W/Mk^{2}s.

CONCLUSION

In the present study, the electronic, elastic, thermodynamic and transport properties of half- Heusler X(X=Co, Rh and Ir)MnAs have been treated using the DFT associated to general gradient approximation.

The elastic constants confirm the material ductile nature with stability in cubic phase C_{1b}. The studied materials have a high Debey temperature (600 °K) at a pressure of 0 GPa.

The thermal properties including the heat capacities C_v and C_p and the thermal expansion coefficient have been studied using the quasi harmonic Debey model in the range of pressure 0 to 25 GPa and of temperature 0 à 900 °K, show that the CoMnAs compound has high values of expansion coefficient with regard to the other compounds. The transport properties have been determined by means of BoltzTraP code.

The CoMnAs materiel presents a high thermoelectric parameter such that Seebeck coefficient, the power and the merit factors. Contrarily, The IrMnAs compounds show weak values for these parameters.

These results could offer a useful reference for the development of thermoelectric material based on XMnAs.

ORCID IDs

Amraoui Rabie, https://orcid.org/0000-0001-9256-488X

REFERENCES

[1] Enamullah, S.K. Sharma, Sameh, and S. Ahmed, J. Phys. Condens. Matter. **32**, 405501 (2020). https://doi.org/10.1088/1361-648X/ab96f0

[2] R. De Groot, F. Mueller, P. Van Engen, and K. Buschow, New class of materials: halfmetallic ferromagnets, Phys. Rev. Lett. **50**, (25) (1983) 2024. https://doi.org/10.1103/PhysRevLett.50.2024

[3] S. Chibani, O. Arbouche, M. Zemouli, Y. Benallou, K. Amara, N. Chami, M.Ameri, and M. El Keurti, First-principles investigation of structural, mechanical, electronic, and thermoelectric properties of Half-Heusler compounds RuVX (X= As,P, and Sb), Comput. Condens. Matter, **16**, e00312 (2018). https://doi.org/10.1016/j.cocom.2018.e00312

[4] F. Benzoudji, O. Miloud Abid, T. Seddik, A. Yakoubi, R. Khenata, H. Meradji, G. Uùgur, S. Uùgur, and H.Y. Ocak, Insight into the structural, elastic, electronic, thermo- electric, thermodynamic and optical properties of MRhSb (MDTi, Zr, Hf) half Heuslers from ab initio calculations, Chinese Journal of Physics, **59**, 434 (2019), https://doi.org/10.1016/j.cjph.2019.04.009

[5] A. Amudhavalli, R. Rajeswarapalanichamy, K. Iyakutti, and A.K. Kushwaha, First principles study of structural and optoelectronic properties of Li based half Heusler alloys, Computational Condensed Matter, **14**, 55 (2018), https://doi.org/10.1016/j.cocom.2018.01.002

[6] F. Aversano, A. Ferrario, S. Boldrini, C. Fanciulli, M. Baricco, and A. Castellero, Thermoelectric Properties of TiNiSn Half Heusler Alloy Obtained by Rapid Solidification and Sintering, J. Mater. Eng. Perform. **27**, 6306 (2018). https://doi.org/10.1007/s11665-018-3735-6

[7] W. Xie, A. Weidenkaff, X. Tang, Q. Zhang, J. Poon, and T.M. Tritt, Recent advances in nanostructured thermoelectric half-Heusler compounds, Nanomaterials, **2**, 379 (2012). https://doi.org/10.3390/nano2040379

[8] J. Ma, V.I. Hegde, K. Munira, Y. Xie, S. Keshavarz, D.T. Mildebrath, C. Wolverton, A.W. Ghosh, and W. Butler, Computational investigation of half-Heusler compounds for spintronics applications, Phys. Rev. B, **95**, 024411 (2017). https://doi.org/10.1103/PhysRevB.95.024411
[9] R. Ahmad, A. Gul, N. Mehmood, Artificial neural networks and vector regression models for prediction of lattice constants of half-Heusler compounds, Mater. Res. Express, **6**, 046517 (2018). https://doi.org/10.1088/2053-1591/aafa9f
[10] S. Chibani, N. Chami, O. Arbouche, K. Amara, A. Kafi, Structural, elastic, electronic and transport properties of CoVX (X=Ge and Si) compounds: A DFT prediction, Computational Condensed Matter, **24**, e00475 (2020). https://doi.org/10.1016/j.cocom.2020.e00475
[11] P. Blaha, K. Schwarz, G.K.H. Madsen, D. Knasnicka, J. Lunitz, R. Laskowski, F. Tran, and L.D. Marks, *WIEN2k, An Augunented Plane Wave Plus Local Orbital Programme for calculating crystal properties*, (Vienna University of Technology, Vienna, Austria, 2001). http://www.wien2k.at/reg_user/textbooks/usersguide.pdf
[12] W. Kohn, L.J. Sham, Self-consistent equations including exchange and correlation effects, Phys. Rev. **140**, A1133 (1965). https://doi.org/10.1103/PhysRev.140.A1133
[13] F.D. Murnaghan, Proc. Natl. Acad. Sci. USA, **30**, 244 (1944). https://doi.org/10.1073/pnas.30.9.244
[14] P. Blaha, K. Schwarz, F. Tran, R. Laskowski, G.K.H Madsen, and D.L. Marks, J. Chem. Phys. 152, 074101 (2020), https://doi.org/10.1063/1.5143061.
[15] M. Born, K. Huang, *Dynamical theory of crystal lattices (international series of monographs on physics*), (Oxford University Press, Oxford, U.K., 1954).
[16] Hill, R. The Elastic Behaviour of a Crystalline Aggregate. Proc. Phys. Soc. Sect. A, **65**, 349 (1952). https://doi.org/10.1088/0370-1298/65/5/307
[17] S.F. Pugh, Philos. Mag. **45**, 823 (1954). https://doi.org/10.1080/14786440808520496
[18] Y. Tian, B. Xu, and Z. Zhao, *Int. J. Refract. Metals Hard Mater.* 33, 93 (2012). https://doi.org/10.1016/j.ijrmhm.2012.02.021
[19] V.I. Razumovskiy, E.I. Isaev, A.V. Ruban, and P.A. Korzhavyi, Intermetallics, **16**, 982 (2008). https://doi.org/10.1016/j.intermet.2008.04.016
[20] N. Arıkan, A. İyigör, A. Candan, Ş. Uğur, Z. Charifi, H. Baaziz, and G. Uğur, Electronic and phonon properties of the full-Heusler alloys X2YAl (X=Co, Fe and Y=Cr, Sc): a density functional theory study, J. Mater. Sci. **49**, 4180 (2014). https://doi.org/10.1007/s10853-014-8113-7
[21] D.-y. Jung, K. Kurosaki, C.-e. Kim, H. Muta, and S. Yamanaka, Thermal expansion and melting temperature of the half-Heusler compounds: MNiSn (M = Ti, Zr, Hf), J. Alloys. Compd. **489**, 328 (2010). https://doi.org/10.1016/j.jallcom.2009.09.139
[22] P. Debye, Ann. Phys. **39**, 789 (1912).
[23] A. Otero-de-la-Roza, D. Abbasi-Pérez, and V. Luaña, Gibbs2: A new version of the quasiharmonic model code. II. Models for solid-state thermodynamics, features and implementation, Comput. Phys. Commun. **182**, 2232 (2011). https://doi.org/10.1016/j.cpc.2011.05.009
[24] A.T. Petit, and P.L. Dulong, Ann. Chim. Phys. **10**, 395 (1819).
[25] E. Bringuier, L'équation de transport électronique de Boltzmann dans les solides et l'approximation du temps de relaxation, European Journal of Physics, **40**, 025103 (2019). https://doi.org/10.1088/1361-6404/aaf5f0
[26] G.K.H. Madsen, and D.J. Singh, BoltzTraP. A code for calculating band-structure dependent quantities, Computer Physics Communications, **175**, 67 (2006). https://doi.org/10.1016/j.cpc.2006.03.007
[27] G. Snyder, in CRC Handbook of Thermoelectrics, ed. D.M. Rowe (Boca Raton: CRC Press, 2006), p. 144.
[28] B. Lenoir, *Thermoélectricité: des principes aux applications*, (Transport, 1990). pp. 1–19.
[29] C.H.L. Goodman, The prediction of semiconducting properties in inorganic compounds, Journal of Physics and Chemistry of Solids, **6**, 305 (1958). https://doi.org/10.1016/0022-3697(58)90050-7
[30] T. J. Seebeck, Abhand. Deut. Akad. Wiss, Berlin, (1822).
[31] F.Z. Fouddad, S. Hiadsi, L. Bouzid, Y.F. Ghrici, and K. Bekhadda, Low temperature study of the structural stability, electronic and optical properties of the acanthite α-Ag2S: Spin-orbit coupling effects and new important ultra- refraction property, Materials Science in Semiconductor Processing, **107**, 104801 (2020). https://doi.org/10.1016/j.mssp.2019.104801
[32] P.F. Taylor, and C. Wood, *Advan. Energy Conversion,* **1**, 141 (1961). https://doi.org/10.1016/0365-1789(61)90023-6
[33] A.I. Ioffe, *Энергетические основы термоэлектрических батарей полупроводников* [*Energeticheskie osnovi termoelektricheskih battery poluprovodnikov*], (Academy of Science of the USSR, Moscow, 1949).

ДОСЛІДЖЕННЯ СТРУКТУРНИХ, ПРУЖНИХ, ТЕПЛОВИХ ТА ТРАНСПОРТНИХ ВЛАСТИВОСТЕЙ ПОТРІЙНИХ СПОЛУК X(X=Co, Rh та Ir)MnAs, ОТРИМАНИХ МЕТОДОМ DFT

Салім Кадрі[a], Тураб Мохамед[b], Беркані Махієддіне[c], Амрауі Рабіє[d], Борджиба Зейнеб[d]
[a]Лабораторія динамічних двигунів та віброакустичної лабораторії, Університет М'Хамеда Бугари в Бумердесі
[b]Факультет технологій, Університет М'Хамеда Бугари, Сіте Франц Фанон, Бумердес 35000-Алжир
[c]Лабораторія LSELM, Університет Баджі Мохтар Аннаба, Аннаба 23000, Алжир
[d]Лабораторія фізики матеріалу - L2PM, 8 травня 1945 р. Університет Гельми, Алжир

Теорія функціональної щільності (DFT) з апроксимацією узагальненого градієнта використовується для дослідження пружних, термодинамічних і транспортних властивостей, а також для структурної стабільності потрійних напівгейслерівських сполук X(X=Co, Rh та Ir)MnAs. Це перше прогностичне дослідження цих сполук визначає такі механічні властивості, як стиснення, зсув, модуль Юнга та коефіцієнт Пуассона, не пропускаючи параметрів перевірки природи цих сполук, таких як твердість, анізотропний факт Зенера та тиск Коші. Коефіцієнт П'ю та коефіцієнт Пуассона дозволили визначити пластичну природу цих сполук. Швидкість звуку та температура Дебая цих сполук також була оцінена за пружними константами. Термодинамічні властивості також розраховані для інтервалу тиску від нуля до 25 ГПа. Вплив зміни хімічного потенціалу на коефіцієнт Зеєбека, електричну, теплову та електронну провідність, коефіцієнти потужності та переваги також досліджували для різних температур (300, 600, 900°K), так що ці сплави можуть бути кращими потенційними кандидатами для термоелектричних додатків.

Ключові слова: Напів-Гейслер, DFT, пружність, термоелектричні, транспортні властивості